DOI: 10.21062/mft.2023.090 http://www.journalmt.com

Structural and Mechanical Properties of CuZn30 Cartridge Brass in Real Production Conditions

Jan Luštinec (0000-0001-8764-6514)[1], Miroslav Roško (0009-0001-5386-7471)[2], Vladivoj Očenášek (0000-0002-7817-8701)[1]
[1]SVÚM a. s., Tovární 2053, 250 88 Čelákovice. Czech Republic. E-mail: lustinec@svum.cz, ocenasek@svum.cz
[2]Povrly Copper Industries a. s., Mírová 63, 403 32 Povrly. Czech Republic. E-mail: miroslav.rosko@pci.cz

The paper deals with the technology of production of deep-drawn plates from alpha brass CuZn30. Surface and hidden defects are often observed in these deep-drawn sheets. The research was aimed at reducing the occurrence of these defects and subsequently reducing scrap and increasing the quality of these metallurgical products with a tighter tolerance of the required structural and mechanical properties throughout the length and width of the sheets. The production technology was monitored from the preparation of the batch and casting parameters on the existing operating equipment, through the processing of the ingots by hot and cold rolling, to the recrystallization annealing of the sheets in coils in a hatch furnace and the subsequent continuous pickling and passivation of the final strips. Properties were monitored after each technological operation of production. Specifically, macrostructure, microstructure, microporosity, tensile mechanical properties, and hardness were analysed. The results showed that the chosen production technology has sufficient homogeneity of properties.

Keywords: Brass, CuZn30, Production Technology, Mechanical Properties, Structure

1 Introduction

1.1 Properties of brass CuZn30

Brass CuZn30 (CW505L) belongs to deep-drawn brasses. The chemical composition of CuZn30 brass according to ČSN EN 1652 is given in Tab. 1. The CuZn30 brass has excellent cold working, excellent mechanical properties and remarkable flexural strength [1-8].

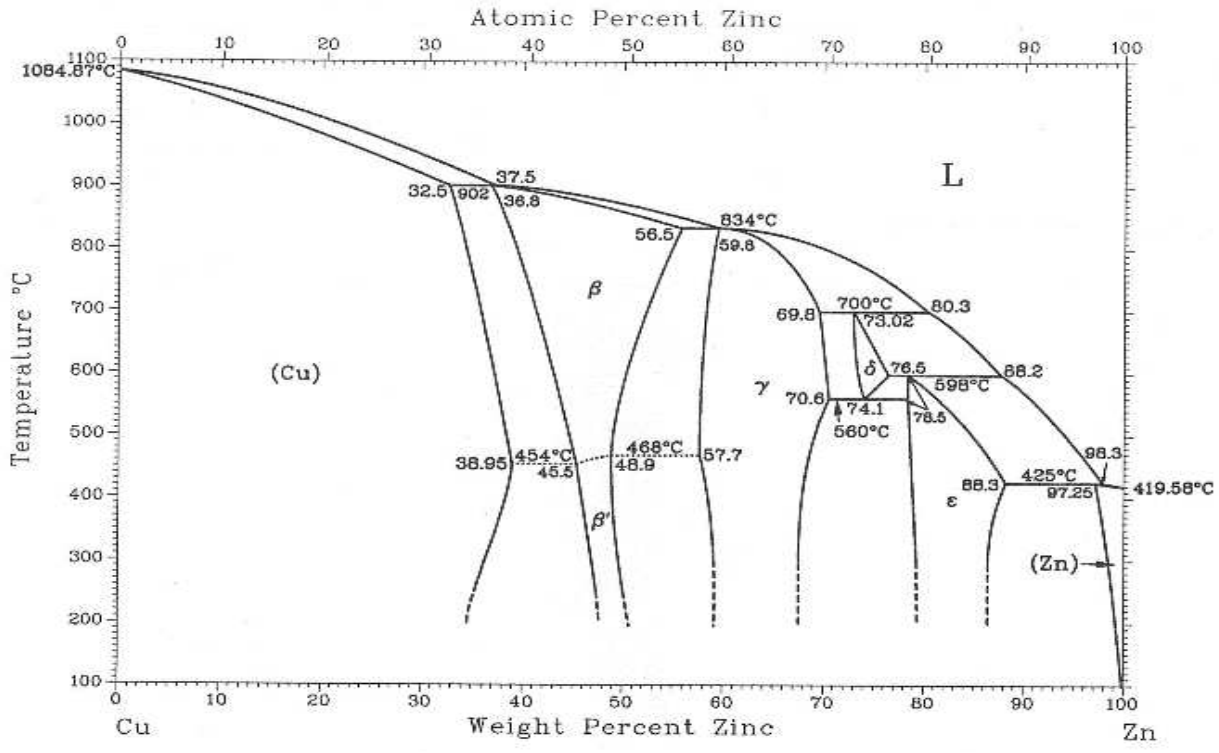

***Fig. 1** Phase diagram Cu-Zn [10]*

Tab. 1 *Chemical composition of brass CuZn30 [9]*

	Cu	Al	Fe	Ni	Pb	Sn	Zn	other
min.	69.0	-	-	-	-	-	Rem	-
max.	71.0	0.02	0.05	0.3	0.05	0.1	-	0.1

Brass CuZn30 is commonly used in the arms industry (e.g. cartridges), in electrical engineering and electronics (e.g. electrical contacts, fasteners), in the automotive (e.g. decorative elements and other components for cars), in the construction industry and as consumer goods (e.g. decorations) [1-8].

The binary diagram of copper and zinc (Fig. 1) shows that zinc and copper form a substitutional solid solution α(Cu). The phase diagram shows the maximum zinc solubility, which is 39 % at 456 °C. As the temperature increases, the solubility of zinc decreases to 32.5 % at 903 °C. The α phase has a face-centred cubic structure and thus good plastic properties when the phase is deformed around room temperature. The β phase, which is well hot-formable, has a body-centred cubic structure and is found in brasses with more than 38 % Zn [1,2,3,10].

The effect of zinc on the strength and ductility of brass is shown in Fig. 2, suggesting the increase of brass strength and ductility with increasing zinc content. The brass reaches maximal ductility at a zinc content of 32 % and its maximal strength at a zinc content of 46 % [1].

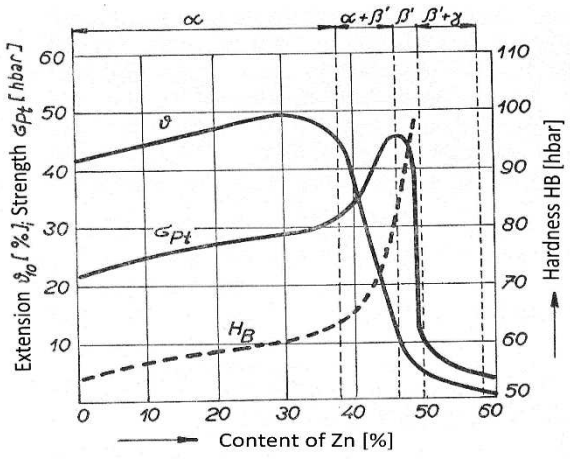

Fig. 2 *Effect of zinc on the mechanical properties of brass [1]*

1.2 Technology of sheet metal production

The production of CuZn30 brass involves several steps, including smelting from pure raw materials, i.e. pure copper and pure zinc, or smelting with the addition of CuZn30 brass scrap. After melting the raw materials, ingots of 180x630x4000 mm are cast from the smelter at a temperature of 1080 – 1130 °C and with a speed of 12 – 16 cm.min^{-1}. The used crystallizer is a single circuit with a vibrating table. The surface is covered with covering salts or synthetic carbon during the melting and casting. Then, the ingots are heated in a step furnace to a rolling temperature in the range of 820 – 840 °C. The ingots are gradually hot-rolled until reaching a thickness of approximately 15 mm. Subsequently, these rolls were milled from both sides. The next step in production is cold rolling to the final sheet thicknesses, i.e. 3.0 – 3.2 mm. Rolling is repeated several times until the required thickness is reached. After the cold rolling, recrystallisation annealing is done in hatch furnaces at 485 °C for 12 hours, followed by pickling and passivation of the final sheets.

Research papers [4-6] dealt with the recrystallization annealing of CuZn30 brass. Combinations of different temperatures and degrees of deformation were the subject of investigations. The conclusions in these works coincide with the temperature chosen for our work, which was based on manufacturing practice.

In current articles, porosity is assessed by image analysis [11] or computed tomography [12]. Alternatively, it is measured by hydrostatic weighing [13]. In this paper, the image analysis method was chosen.

2 Methods and equipment

During the research, different methods of sample preparation were used, which were analysed on laboratory equipment. The following paragraphs summarise the analysis methodology.

Sample preparation included surface milling and subsequent etching in nitric acid (HNO_3) for macrostructural analysis.

The metallographic sections for microstructural analysis were prepared by pressing the samples on a press (CitoPress-10) and then polishing on a TegraPol-35. The samples were etched ($K_2Cr_2O_7$, H_2SO_4, H_2O) to highlight the microstructure, which was analysed on an Axio Observer.Z1m microscope. Porosity was assessed by image analysis in Olympus Stream Desktop software. Furthermore, microstructural analyses were performed with an energy-dispersive X-ray spectroscopy (Bruker XFlash Detector 5010) on a scanning electron microscope (EVO MA10).

The tensile mechanical properties were measured on an Instron 5500R. A tensile speed of 0.015 mm.min^{-1} was selected up to a strain of 1 % and then was set to 0.402 mm.min^{-1}.

Vickers hardness (HV5) was measured on metallographic sections on a hardness tester (Qness 30CHD Master+).

ISSN 1213–2489
e-ISSN 2787–9402

3 Experiment and results

3.1 Cast ingots

In total, five ingots were cast for the analysis, three were made by the standard process used for casting ingots during production and the remaining two were prepared from a wet batch. The cross-sections were taken from both ends of each cast ingot and etched to highlight the macrostructure for the analysis.

The character of the macrostructure of ingots depends mainly on the place of collection. The macrostructure of ingot beginnings differs significantly from the macrostructure of ingot ends.

The macrostructure of the beginnings of all the ingots studied has essentially the same character as shown schematically in Fig. 3. Columnar grains from the two longer opposite sides meet in the half-plane. These columnar grains growing from the lateral (shorter) sides form characteristic triangles terminated by triple points. Areas of fine equiaxial grains have been observed near the surface of the long sides, usually about midway along their length. An example of the macrostructure of the beginning of an ingot is shown in Fig. 4.

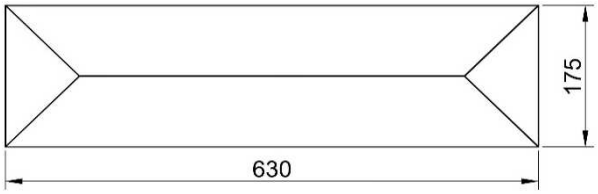

Fig. 3 *Schematic character of macrostructures of cast ingot beginnings*

Fig. 4 *Macrostructure of the beginning of the cast ingot*

The macrostructure of the ends of the ingots has the character shown schematically in Fig. 5. In the centre of the casting, a region with equiaxial grains is observed. Also, areas of fine equiaxial grains are near the surfaces of the long sides. An example of the macrostructure of the ingot end is shown in Fig. 6.

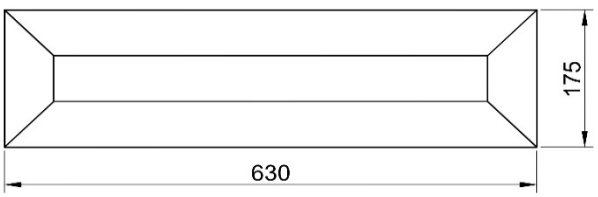

Fig. 5 *Schematic character of macrostructures of cast ingot ends*

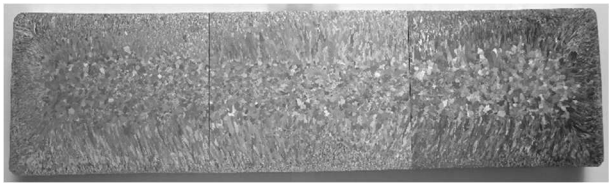

Fig. 6 *Macrostructure of the end of the cast ingot*

Furthermore, the microstructure at several locations of the cross-sections of the cast ingots was evaluated. The microstructure of the equiaxial grain region is shown in Fig. 7 and the triple point region is shown in Fig. 8. In the region of equiaxial grains near the surface, the grain size ranged from 250 to 1000 μm for all cross-sections. The size of dendrites ranged from 60 to 90 μm. In the triple point region, grain size was greater than 1000 μm for all sections. Dendrite size ranged from 50 to 130 μm. No close association of grain and dendrite size was observed at each location of the cross-sections taken from the beginnings and ends of the castings with the batch and casting parameters.

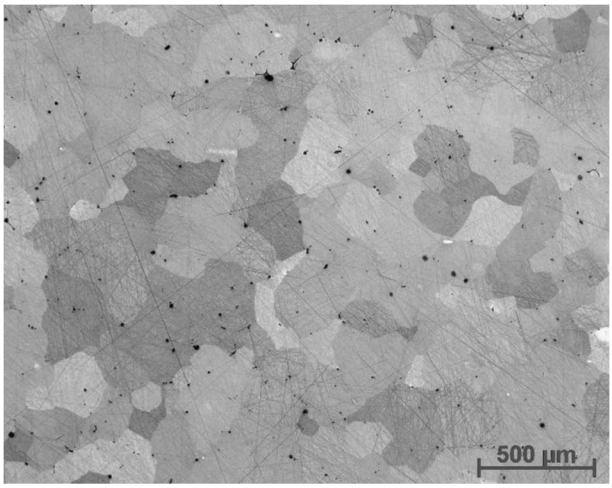

Fig. 7 *Microstructure of the fine-grained part near the surface*

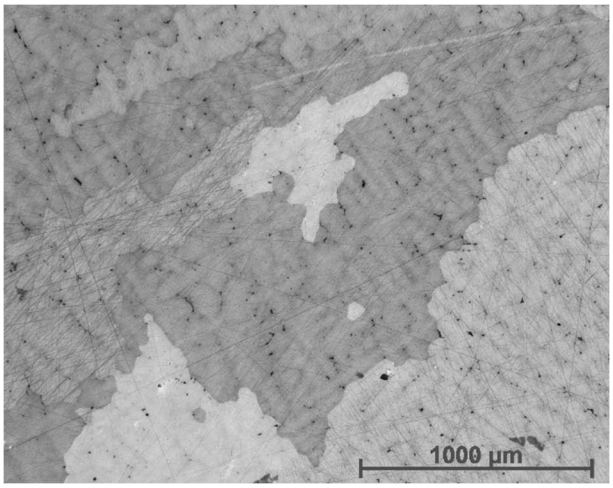

Fig. 8 *Microstructure at the triple point*

Another investigated property was microporosity, i.e. the areal density of relatively small pores (<10 μm). The porosity was evaluated at five random locations with 2.5x2.5 mm dimensions on each sample. The microporosity was assessed by image analysis and was determined as a percentage. Only microporosity was assessed and any macropores, i.e. various voids and stagnation caused by uneven solidification of the melt, were not included in the evaluation. The microporosity represents the amount of microporus in the melted metal and subsequently, in the solidified metal (cast). Although the measurement itself is burdened by a large measurement error, several useful conclusions can be made from the performed analyses. Microporosity is always significantly greater at the beginning of casting for all tested castings compared to the ingot end, where the microporosity is significantly smaller. The effect of a wet batch on microporosity was undetected.

3.2 Hot rolling and hot-rolled forgings

The next investigated technological step in production is the hot rolling of cast blocks. Cross-sections were analysed in two locations of the hot-rolled forgings concerning the shape of the lateral sides.

The shaping of the sides of hot-rolled forgings depends on the lateral spread of the hot-rolled forgings during rolling. This spreading depends mainly on the friction between the surface of the hot-rolled forgings and the rolls. The results showed that the shape of the hot-rolled forgings sides is variable. The character of the lateral sides can be classified into three types: concave, straight and convex (Fig. 9). No distinct regularity in their formation has been found. It was common for one sample at a distance of 500 mm to change from slightly concave to strongly convex and vice versa. The results eliminated the possibility that the sides of the hot-rolled forgings could produce folds, leading to discontinuities of the final deep-drawn bands at their edges.

Fig. 9 *Hot-rolled forgings and their side edge types*

Samples were taken from the central part of the hot-rolled forgings in the rolling and perpendicular directions for microstructural analysis. The microstructure was analysed for grain size and the presence of unwanted intermetallic phases and inclusions. The grain size of all studied hot rolled forgings ranged from 54 to 64 μm. The microstructure is documented in Figs. 10 and 11. Sparsely distributed dark phases were detected in the structure of the samples. Subsequently, these dark phases were analyzed by energy-dispersive X-ray spectroscopy (EDS) in a scanning electron microscope (SEM). The distribution maps of selected elements (Cu, Zn and S) were determined for selected phases (Fig. 12) and also the chemical composition was measured. The analysis of the EDS results indicated that the inclusions were ZnS. Their occurrence to a greater extent is probably responsible for the presence of the blistering of the deep-tension bands. These defects significantly reduce the quality of these strips and therefore, measures were incorporated into the technological process to prevent ZnS formation.

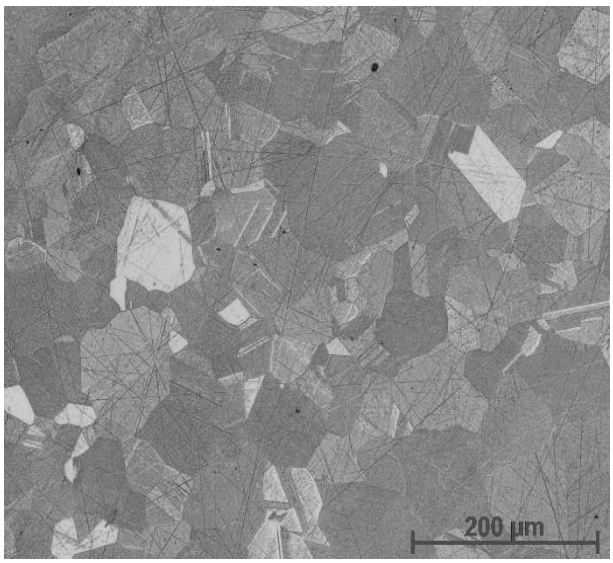

Fig. 10 *Microstructure of hot-rolled forging in cross section per rolling direction*

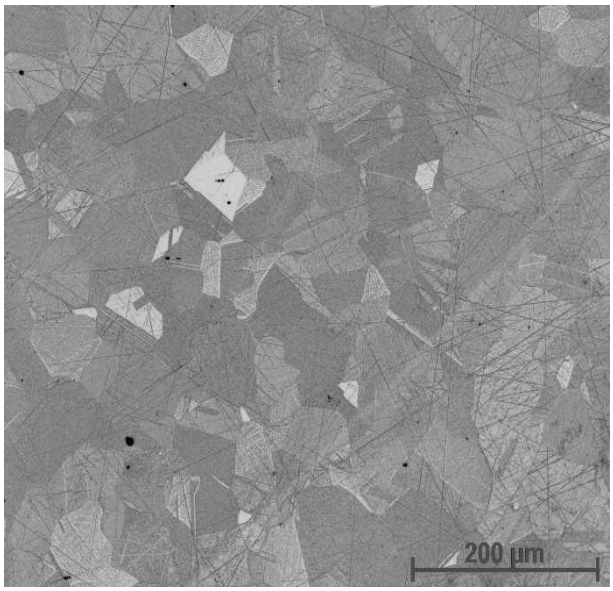

Fig. 11 *Microstructure of hot-rolled forging in the rolling direction*

ISSN 1213–2489
e-ISSN 2787–9402

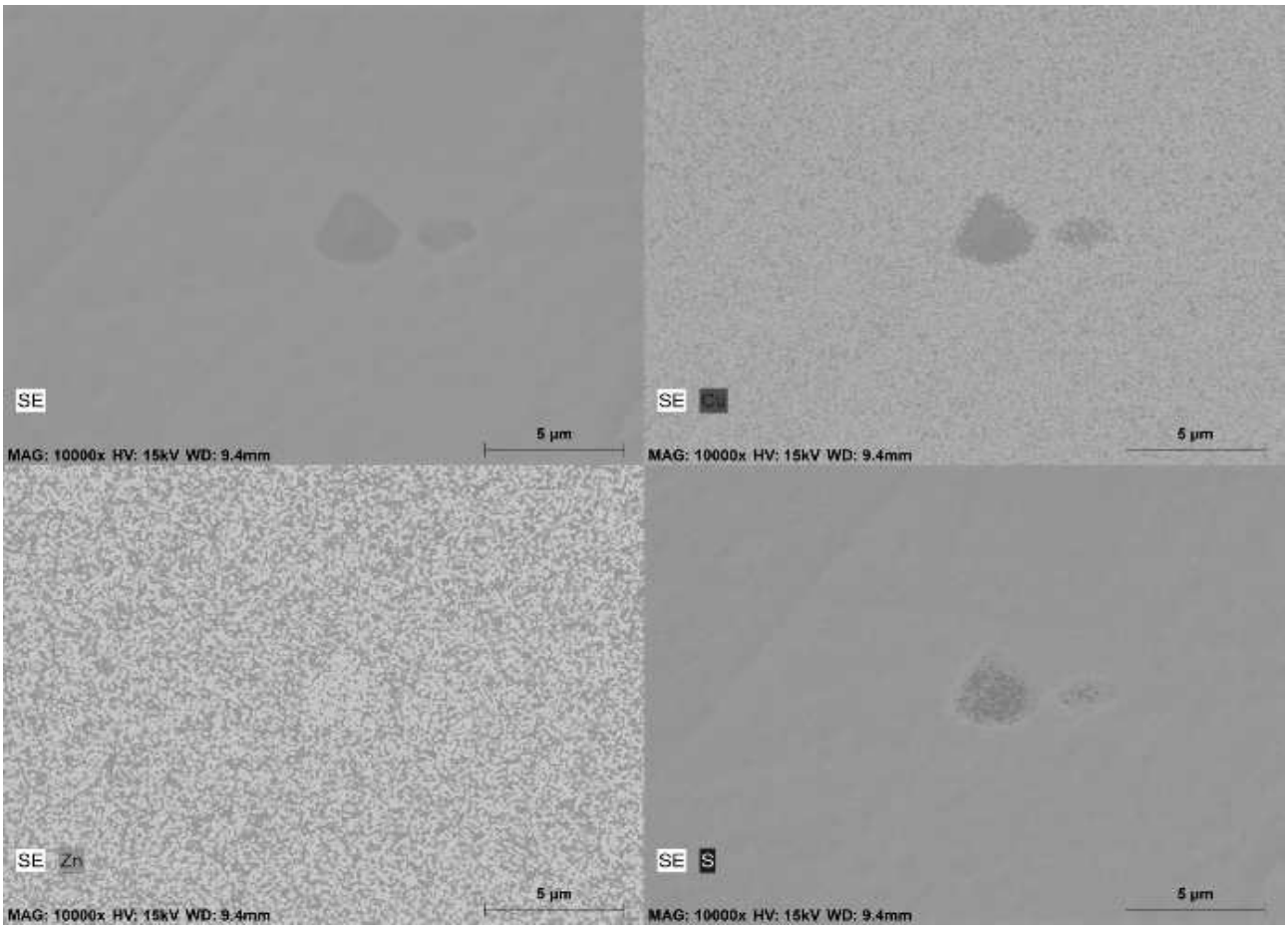

Fig. 12 *Distribution maps (Cu, Zn and S) of hot-rolled forging*

3.3 Cold rolling and final sheets

The hot-rolled forgings were first milled on both sides. Subsequently, they were cold rolled with followed recrystallization annealing. The analyses aimed to verify the optimum setting of the existing technological procedures for the production of CuZn30 sheets. The properties of the sheets were measured before and after recrystallization annealing for comparison.

The structural analysis showed that the structure of all cold rolled sheets consisted of grains elongated in the rolling direction (Figs. 13 and 14). In the longitudinal section, the structure showed numerous deformation bands, deformation twins, as well as so-called shear bands, typical for brasses rolled at high reductions above 70 %. These structures correspond to the cold rolled condition [4,14,15]. Zinc sulfides ZnS stretched in the forming direction, were present in the structure.

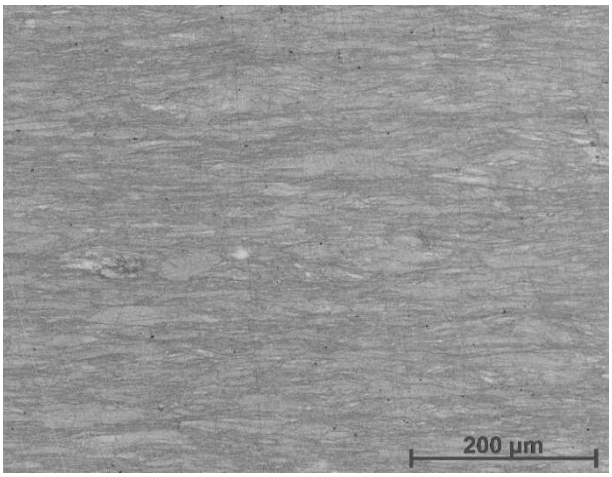

Fig. 13 *Microstructure of rolled sheet before recrystallization annealing, cross section*

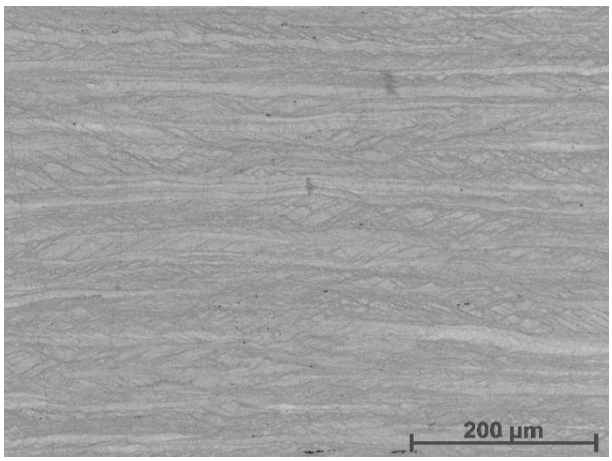

Fig. 14 *Microstructure of rolled sheet before recrystallization annealing, longitudinal section*

The structure of all annealed sheets was recrystallized with annealing twins. The grains were equiaxial, as can be seen from the images of the structure in longitudinal and perpendicular metallographic sections to the rolling direction (Figs. 15 and 16). The structures correspond to typical recrystallization structures of CuZn30 brass [4,14,15]. No differences in the structure among the centres and edges, and the beginnings and ends of the analyzed sheets were found. In conclusion, the structures of the individual sheets were practically the same throughout the length and width of the sheets.

In addition to the structure, mechanical properties were also investigated. The mechanical properties of the sheets after rolling without recrystallization annealing were determined on three test bars taken in the rolling direction in the central part of the sheet. In the tensile test, the tensile strength R_m and the ductility A_{50} were obtained. Similarly, the mechanical properties after recrystallization annealing were also determined, obtaining also the tensile strength R_m and the ductility A_{50}.

The hardness of unannealed and annealed sheets was measured on metallographic cross-sections.

The average values of the mechanical properties of all the examined samples are in Tab. 2. These values correspond well with those commonly achieved for cartridge brass sheets [4,6].

It was verified that the selected production technology is optimal, especially the annealing modes concerning the degree of deformation hardening by cold rolling with a reduction of about 80 %.

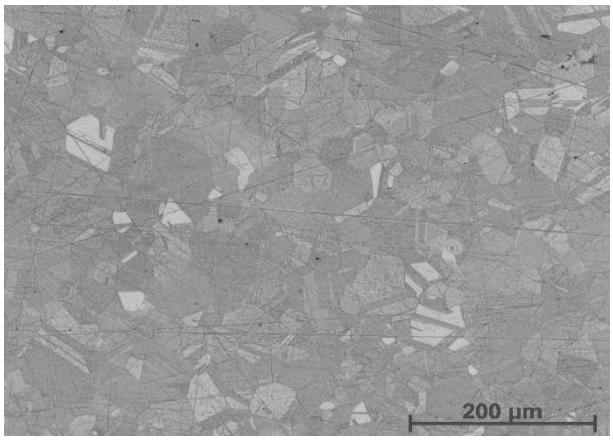

Fig. 15 *Microstructure of rolled sheet after recrystallization annealing, cross section*

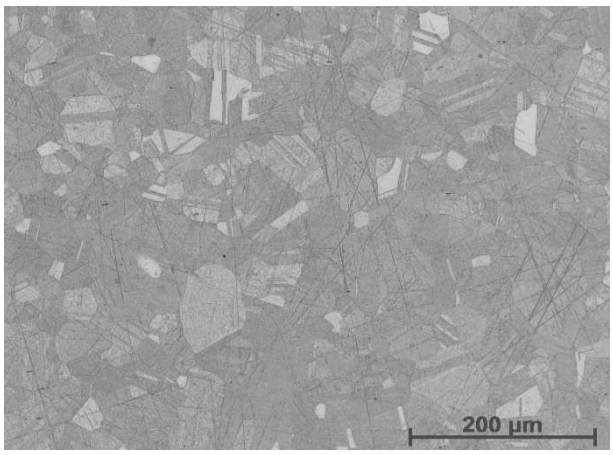

Fig. 16 *Microstructure of rolled sheet after recrystallization annealing, longitudinal section*

Tab. 2 *Mechanical properties of cold rolled sheets before and after recrystallization annealing*

	R_m [MPa]	A_{50} [%]	HV 5 [1]	d_m [mm]
sheets before recrystallization annealing	692 ± 9.6	1.6 ± 2.0	208 ± 5.1	-
sheets after recrystallization annealing	328 ± 6.5	60.4 ± 7.7	71 ± 3.8	0.038 – 0.044

4 Conclusions

In this work, CuZn30 cartridge brass was detail investigated during each step of the production process to evaluate the influence of the specific production procedures on the material properties. The main focus was on the critical parts of the production, especially on casting, hot rolling and final thermo-mechanical processing. The production process was optimised to achieve the desired structure and mechanical properties over the entire sheets in the soft state.

The results of the structure and mechanical properties on samples taken from different locations of the final sheets studied showed sufficient homogeneity of properties along their length and width. The microporosity caused by melt flow is greater at the beginning of the casting process. Any change of microporosity caused by using the wet batch was undetected. ZnS inclusions are present in the structure in areas that are deforming and orienting in the rolling direction during forming.

It was shown that the chosen production technology, i.e. annealing modes concerning the degree of deformation hardening by cold rolling, was optimally adjusted to achieve the desired structural and mechanical properties.

Acknowledgement

The results presented in this paper were created with the financial support of MPO ČR within the framework of the project CZ.01.1.02/0.0/0.0/20_321/0024505.

References

[1] PÍŠEK, F., JENÍČEK, L., RYŠ, P. (1973). *Nauka o materiálu I/3*, ACADEMIA, Prague. ISBN 21-111-73

[2] SEDLÁČEK, V. (1979). *Neželezné kovy a slitiny*, SNTL – Státní nakladatelství technické literatury, Prague. ISBN 04-414-79

[3] SEDLÁČEK, V. (1957). *Neželezné kovy – Hutnické výrobky a jejich použití*, SNTL – Státní nakladatelství technické literatury, Prague.

[4] OZGOWICZ, W., KALINOWSKA-OZGOWICZ, E., GRZEGORCZYK, B. (2010). The microstructure and mechanical properties of the alloy CuZn30 after recrystallizion annealing. In: *Journal of Achievements in Materials and Manufacturing Engineering*, Vol. 40, No. 1. ISSN 2300892X

[5] MUHAMMED, A., ABED, A., MUSTAFA, M. A. (2012). Effects of recrystallization temperature on the mechanical properties of CuZn30 alloy. In: *First National Conference for Engineering Sciences (FNCES 2012)*, pp. 1 – 6. Iraq. ISBN 978-1-4673-5032-7

[6] KLEIN, J. (2016). Recrystallization Behavior of 70/30 Brass. In: *Physical and mechanical properties of materials*, University of Illinois at Chicago. Chicago.

[7] BEZECNY, J., DUBEC, A. (2016). Metallographic and finite element evaluation of plastic deformation during the forming process of cartridge brass casings. In: *Procedia Engineering*, Vol. 136, pp. 137 – 142. ISSN 1877-7058

[8] MUTLU, M., KARAKAŞ, A., KUŞDEMIR, H., KOLTAN, U. K., YALÇINKAYA, T. (2023) Flow forming and recrystallization behaviour of CuZn30 alloy. In: *Materials Research Proceedings*, Vol. 28, pp. 1021 – 1028.

[9] *ČSN EN 1652 Měď a slitiny mědi – Desky, plechy, pásy a kotouče pro všeobecné použití* (2000), Český normalizační institute, Prague.

[10] BAKER, H. (1999). *ASM Handbook, Volume 3, Alloy Phase Diagrams*, ASM International, Ohio. ISBN 0-87170-381-5

[11] HREN, I., LUŇÁK, M.., KUŚMIERCZAK, S. (2020). The formation and elimination of the negative influence of porosity on the properties of the alloy castings AlSi10Mg. In: *Manufacturing Technology*, Vol. 20, No. 2, pp. 170 – 176. ISSN 1213-2489

[12] KUCHARIKOVÁ, L., TILLOVÁ, E., KRITIKOS, M., UHRÍČIK, M., ŠVECOVÁ, I. (2020). Usage of a non-destructive testing technology for assessment of porosity in aluminium casts alloys. In: *Manufacturing Technology*, Vol. 20, No. 5, pp. 632 – 638. ISSN 1213-2489

[13] ZYSKA, A., BOROŃ, K. (2021). Comparison of the Porosity of Aluminum Alloys Castings Produced by Squeeze Casting.In: *Manufacturing Technology*, Vol. 21, No. 5, pp. 725 – 734. ISSN 1213-2489

[14] WALKER, H. L. (1945). Grain sizes produced by recrystalization and coalescence in cold-rolled cartridge brass. In: *University of Illinois Bulletin*, Vol. 43, No. 21, University of Illinois Urbana.

[15] VANDER VOORT, G. (2015). Deformation and Annealing of Cartridge Brass. https://vacaero.com/information-resources/metallography-with-george-vander-voort/1440-deformation-and-annealing-of-cartridge-brass.html